

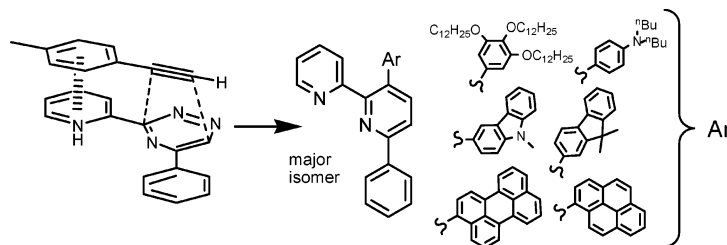
A Rational Protocol for the Synthesis of Arylated Bipyridine Ligands via a Cycloaddition Pathway

Stéphane Diring,[†] Pascal Retailleau,[‡] and Raymond Ziessel^{*,†}

Laboratoire de Chimie Moléculaire, Centre National de la Recherche Scientifique (CNRS),
École de Chimie, Polymères, Matériaux (ECPM), 25 rue Becquerel,
67087 Strasbourg Cedex 02, France, and Laboratoire de Cristallogénie, ICSN-CNRS,
Bât 27-1 avenue de la Terrasse, 91198 Gif-sur-Yvette, Cedex, France

ziessel@chimie.u-strasbg.fr

Received September 14, 2007



A generic design principle for the preparation of a variety of substituted phenyl–polypyridine ligands is described. These ligands are readily prepared by a regioselective [4+2] cycloaddition between electron-deficient dienes, such as 2,6-disubstituted-1,3,4-triazines, and ethynyl–arenes or ethynyl–alkanes. Exceptional reactivity is found with electron-rich dienophiles bearing ethynylgallate or ethynylphenyldibutylamino groups. Two regioisomers are formed, the meta being preferred due to favorable π – π interactions in the transition state, while the para isomers are formed in low yields in most cases. The use of *tert*-butylacetylene or *N,N*-dimethylamino-2-propyne, however, drives the reaction exclusively to the para isomer. Di-*N,N*-dibutylaminophenyl or isoquinoline ligands can also be produced in a single step by reverse Diels–Alder reactions. Cross-coupling reactions of iodo-substituted ligands or their platinum(II) complexes under Pd(0) catalysis gives branched ligands and complexes bearing paraffin chains, electron-donor or electron-acceptor groups. The use of a chloro–Pt(II) complex of an iodo-functionalized ligand allows both halogens to be replaced by ethynyl groups by using different catalysts. This methodology readily accommodates various functional groups and has been successfully extended to systems containing a variety of donor/acceptor frameworks. All ligands strongly absorb in the near-UV and luminesce in solution at rt with quantum yields ranging from 0 to 66%. Excited state lifetimes are in the nanosecond range and the solvent effects are in keeping with singlet excited states mixed with charge-transfer character. As deduced from spectroscopic and electrochemical studies, the di-*n*-butylamino derivatives are strong reductants in the excited state.

Introduction

The construction of sophisticated ligands is a primary stimulus for the production of novel transition metal complexes, some of which adopt quite exotic structures.^{1–4} Many applications of the resultant new materials are foreseen in areas such as

molecular electronics, opto-electronics, chemical sensing and analysis, and photovoltaics.^{5–8} The necessary ligands, however,

[†] École de Chimie, Polymères, Matériaux (ECPM).

[‡] Laboratoire de Cristallogénie, ICSN-CNRS.

(1) Munakata, M.; Wu, L. P.; Kuroda-Sowa, T. *Adv. Inorg. Chem.*, **1999**, 46, 173.

(2) Piguet, C. *J. Incl. Phenom. Macrocycl. Chem.* **1999**, 34, 361.

(3) (a) Ziessel, R.; Matt, D.; Toupet, L. *Chem. Commun.* **1995**, 2033. (b) Romero, F. M.; Ziessel, R.; Dupont-Gervais, A.; Van Dorsselaer, A. *Chem. Commun.* **1996**, 551. (c) El-ghayoury, A.; Douce, L.; Skoulios, A.; Ziessel, R. *Angew. Chem., Int. Ed.* **1998**, 37, 2205.

(4) (a) Hill, C. L.; Zhang, X. *Nature* **1995**, 373, 324. (b) Collier, C. P.; Wong, E. W.; Belohradsky, M.; Raymo, F. M.; Stoddart, J. F.; Kuekes, P. J.; Williams, R. S.; Heath, J. R. *Science* **1999**, 285, 391.

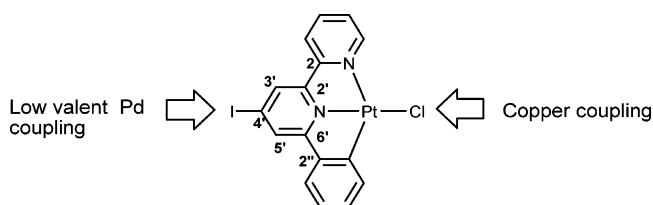
(5) Lehn, J. M. in *Supramolecular Chemistry, Concepts and Perspectives*; VCH: Weinheim, Germany, 1995.

have commonly been obtained via Skraup,⁹ Krönke,¹⁰ or Friedländer¹¹ condensations, which usually provide symmetrically substituted species.¹² Development, more recently, of methods for the synthesis of unsymmetrical oligopyridines (bipyridines, terpyridines, quaterpyridines, quinquepyridines, hexapyridines, and branched derivatives) has attracted considerable attention because of merits including the ready availability of starting materials, good regioselectivity, and facile separation of the products.¹³ While these [4+2] cycloaddition reactions of electron-deficient dienes, such as 1,2,4,5-tetrazines or 1,2,4-triazines, do require the use of dienophiles of complementary electronic character, such as ynamines which guarantee sufficient overlap of the frontier orbitals,¹⁴ it is known that simple organotin alkynes, for example, offer good reactivity and new possibilities for the synthesis of polypyridine ligands.^{13a}

There is a general agreement that additional functionalization of the periphery of a ligand may provide even more interesting complexes and it has been recognized in particular that the use of 6-aryl-2,2'-bipyridine and its derivatives leads to orthometallation reactions with transition metal salts. Neutral Pt(II) complexes with intriguing structural and spectroscopic properties have been prepared on this basis.¹⁵ Some of these have found applications in light emitting devices due to their good stability, bright phosphorescence, and processability.¹⁶ The incorporation of transition metals such as Pt(II) is crucial in order to relax the spin selection rules for phosphorescence through spin-orbit coupling.¹⁷ This has proven to be also important in the design of light-emitting diodes,¹⁸ nonlinear optical materials,¹⁹ and conductance switches.²⁰

Despite intense interest, progress in this field has been hampered by the availability of conveniently prepared starting materials of adequate stability. Conceptually, the preparation of functionalized, potentially tridentate ligands by a retro Diels-Alder reaction is a highly attractive method for the linking of electron-donor or -acceptor units, paraffin chains for the engineering of soft materials, and functional groups suitable for the assembly and stabilization of highly organized edifices.

CHART 1



Essential for this purpose are robust and easily activated molecules that react under mild conditions and exhibit favorable regioselectivity when cross-coupling is envisaged. These requirements may be met by complexation of 4'-iodo-6'-phenyl-2,2'-bipyridine to Pt(II), enabling the linkage of an alkynyl group either in place of the iodo-substituent using Pd(0) catalysis or to the metal center using a Cu(I) cross-coupling reaction (Chart 1).

The use of tributyl(ethynyl)tin as a dienophile in high-temperature [4+2] cycloadditions with electron-deficient heterodienes, such as 1,2,4-triazines,²¹ illustrates the potential of such reactions for the construction of a variety of different dissymmetrically substituted 2,2'-bipyridine ligands. Herein, we report the successful extension of this chemistry by the use of different ethynyl-substituted templates affording 3- or 4-aryl-6-phenyl-2,2'-bipyridine ligands, readily converted to stable Pt(II) complexes. This chemistry generally produces good to excellent yields, tolerates various functional groups (donors and acceptors), and has been successfully extended to systems containing polyaromatic frameworks. The viability of the procedure outlined in Chart 1 has been demonstrated in several cases.

Results and Discussion

As part of our research program on the design and construction of novel ligands bearing various appended functions,²² we planned to develop an efficient method for the synthesis of aryl-substituted bipyridine ligands. Earlier work on LEGO systems provided appropriate inspiration.¹³ Condensation of 2-cyanopyridine with hydrazine gave the corresponding carboxamidrazone which, by condensation with 2-phenylglyoxal, afforded the 2,6-disubstituted-1,3,4-triazine **1** as major isomer, as unambiguously confirmed by NMR spectroscopy (Scheme 1). As found earlier with monosubstituted glyoxals, the formation of the 2,6-disubstituted isomer is strongly favored over that of the 2,5-disubstituted isomer owing to the greater nucleophilicity of the N-NH₂ fragment.²³

Thermal condensation of 4-ethynyltoluene with the 6-phenyl-2-pyridyl-1,3,4-triazine **1** provided compound **2a** as the major and more polar product, and **2b** as the minor and less polar product (Scheme 1). Unambiguous establishment of the isomeric forms was provided by ¹H NMR spectroscopy and X-ray structure determinations on single crystals. Aromatic proton resonances in the NMR spectra of **2a** and **2b** are shown in Figure 1a.

(21) Sauer, J.; Heldmann, D. K.; Pabst, G. R. *Eur. J. Org. Chem.* **1999**, 313.

(22) (a) Ziessele, R.; Bäuerle, P.; Ammann, M.; Barbieri, A.; Barigelli, F. *Chem. Commun.* **2005**, 802. (b) Goeb, S.; De Nicola, A.; Ziessele, R.; Sabatini, C.; Barbieri, A.; Barigelli, F. *Inorg. Chem.* **2006**, 45, 1173. (c) Harriman, A.; Izzet, G.; Goeb, S.; De Nicola, A.; Ziessele, R. *Inorg. Chem.* **2006**, 45, 9729.

(23) Neunhoeffer, H. In *Comprehensive Heterocyclic Chemistry I*; Katritzky, A. R., Rees, C. W., Eds.; Pergamon Press: Oxford, UK, 1984; Vol. 3, pp 385–456.

(6) Constable, E. C. In *Metal and Ligand Reactivity*; VCH: Weinheim, Germany, 1996.

(7) Bignozzi, C. A.; Schoonover, J. R.; Scandola, F. *Prog. Inorg. Chem.* **1997**, 44, 1.

(8) Ziessele, R. F. *J. Chem. Educ.* **1997**, 74, 673.

(9) (a) Skraup, Z. H. *Ber. Dtsch. Chem.*, **1880**, 13, 2086. (b) Manske, R. H. F.; Kulka, M. In *Organic Reactions; The Skraup Synthesis of Quinolines*; John Wiley & Sons: New York, 1953; Vol. 7, p 59.

(10) Krönke, F. *Synthesis* **1976**, 1.

(11) (a) Thummel, R. P. *Synlett*, **1992**, 1. (b) Cheng, C.-C.; Yan, S.-J. In *Organic reactions; The Friedländer Synthesis of Quinolines*; John Wiley & Sons: New York, 1982; Vol. 28, p 37.

(12) (a) Thummel, R.; Chamchoumis, C. M. *Adv. Nitrogen Heterocycl.* **2000**, 4, 107. (b) Chelucci, G.; Thummel, R. P. *Chem. Rev.* **2002**, 102, 3129. (c) Fallahpour, R.-A. *Synthesis* **2003**, 155.

(13) (a) Pabst, G. R.; Sauer, J. *Tetrahedron* **1999**, 55, 5067. (b) Pabst, G. R.; Sauer, J. *Tetrahedron* **1999**, 55, 5047.

(14) Sauer, J.; Sustmann, R. *Angew. Chem., Int. Ed.* **1980**, 19, 779.

(15) Lu, W.; Chan, M. C. W.; Zhu, N.; Che, C.-M.; Li, C.; Hui, Z. *J. Am. Chem. Soc.* **2004**, 126, 7639.

(16) Lu, W.; Mi, B.-X.; Chan, M. C. W.; Hui, Z.; Che, C.-M.; Zhu, N.; Lee, S.-T. *J. Am. Chem. Soc.* **2004**, 126, 4958.

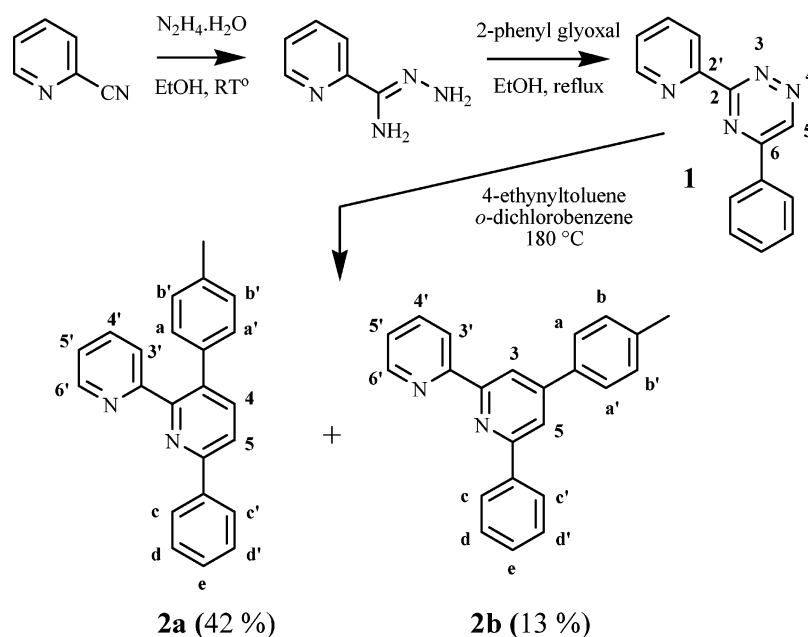
(17) Kober, E. M.; Caspar, J. V.; Lumpkin, R. S.; Meyer, T. J. *J. Phys. Chem.* **1986**, 90, 3722.

(18) (a) Burroughes, J. H.; Bradley, D. D. C.; Brown, A. R.; Marks, R. N.; Mackay, K.; Fried, R. H.; Burns, P. L.; Holmes, A. B. *Nature* **1990**, 347, 539. (b) Holder, E.; Langeveld, B. M. W.; Schubert, U. S. *Adv. Mater.* **2005**, 17, 1109.

(19) Tessler, N.; Denton, G. J.; Fried, R. H. *Nature* **1996**, 382, 695.

(20) Donhauser, Z. J.; Mantooth, B. A.; Kelly, K. F.; Bumm, L. A.; Monnell, J. D.; Stapleton, J. J.; Price, D. W., Jr.; Rawlett, A. M.; Allara, D. L.; Tour, J. M.; Weiss, P. S. *Science* **2001**, 292, 2303.

SCHEME 1



Noteworthy is the AB quartet observed near δ 8 ppm ($J_{AB} = 8.1$ Hz, $\nu_0\delta = 12.7$ Hz) for H4, H5 of the meta isomer **2a**, whereas for the para isomer **2b**, H3 and H5 are split into two simple doublets ($^4J = 1.5$ Hz) at 8.50 and 8.09 ppm. Another key feature is that the doublet at 8.61 ppm assigned to H3' on the outer pyridine ring of the para isomer **2b** is shielded by ~ 1.15 ppm for the meta isomer **2a**, probably influenced by the shielding cone of the tolyl ring. These differences, shown for selected cases in Figure 1, are systematically observed for the series of molecules depicted in Scheme 2.

To confirm the isomer assignments, the two first ligands were characterized by single-crystal X-ray diffraction (Figure 2).

Briefly, in the solid state the nitrogen atoms of the bipyridine moiety lie in a transoid position that minimizes repulsive interactions between the neighboring lone pairs, a situation frequently found in oligopyridine ligands.²⁴ However, while the two pyridine rings of the para isomer **2b** are almost planar (tilt angle of 5.35°), they are strongly tilted (by 56.94°) in the meta isomer **2a** as a consequence of the steric crowding induced by the tolyl fragment. In line with this hypothesis is the large 53.90° tilt angle of the tolyl relative to the central pyridine ring in the meta isomer **2a**, compared to the 30.92° tilt angle found in the para structure **2b**.

To explore the limits of this inverse Diels–Alder reaction we initially chose a variety of acetylenic derivatives such as 4-ethynyltrialkoxycallate,²⁵ 2-ethynyl-9,9-dimethylfluorene,²⁶ and 3-ethynyl-9-methylcarbazole²⁷ because (i) these compounds could be efficiently prepared by Sonogashira protocols, (ii) they are electron-rich dienophiles and thermally stable, and (iii) the resulting compounds **3a/b** to **5a/b** might find useful applications as liquid crystalline materials²⁸ and optically tunable light

emitting complexes.²⁹ Heating these stable ethynyl derivatives in *o*-dichlorobenzene at 180°C provided compounds **3a/b**, **4a/b**, and **5a/b** in acceptable yields (Scheme 2). ^1H NMR spectroscopy showed that in each case the major product was the meta isomer, as initially found with the ethynyltoluene compounds **2a/b**, but the less polar para isomers were also isolated in most cases. The ^1H NMR spectra (see Figure 1b–d) also established the nature of each isomer. When the less thermally stable 1-ethynylpyrene³⁰ and 3-ethynylperylene³¹ derivatives were used in the reverse Diels–Alder condensation, the yields were poor and only the meta isomers **6** and **7** were isolated, with traces of the para isomers only detected by thin-layer chromatography. Interestingly, by using 4-ethynyl-*N,N*-dibutylaminophenyl³² the condensation provided the meta-isomer **8a** in relatively good yield and the para isomer **8b** in modest yield.

To further explore the scope of this synthesis, we examined the reactivity of some other alkynes bearing electron-deficient or bulky substituents on the remote end of the alkyne (Scheme 2). With electron-withdrawing fragments, the reaction proceeded very slowly and no condensation occurred with 2-ethynyl-4,6-dimethoxy-1,3,5-triazine.³³ Here, this was due to the instability of the dienophile. When 4-ethynyl-2,2':6',2''-terpyridine,³⁴ 3,3-dimethylbut-1-yne, or 1-dimethylamino-2-propyne was condensed at high temperature with 6-phenyl-2-pyridyl-1,3,4-triazine, the reaction proceeded smoothly and afforded exclusively the para isomers **9**, **10**, and **11**, respectively.

(28) Camerel, F.; Bonardi, L.; Schmutz, M.; Ziessel, R. *J. Am. Chem. Soc.* **2006**, *128*, 4548.

(29) Montes, V. A.; Pohl, R.; Shinar, J.; Anzenbacher, P., Jr. *Chem. Eur. J.* **2006**, *12*, 4523.

(30) Hissler, M.; Harriman, A.; Khatyr, A.; Ziessel, R. *Chem. Eur. J.* **1999**, *5*, 3366.

(31) Inouye, M.; Hyodo, Y.; Nakazumi, H. *J. Org. Chem.* **1999**, *64*, 2704.

(32) Traber, B.; Wolff, J.; Rominger, F.; Oeser, T.; Gleiter, R.; Wortmann, R. *Chem. Eur. J.* **2004**, *10*, 1227.

(33) Menicagli, R.; Samaritani, S.; Gori, S. *Tetrahedron Lett.* **1999**, *40*, 8419.

(34) Grossshenny, V.; Romero, F. M.; Ziessel, R. *J. Org. Chem.* **1997**, *62*, 1491.

(24) Drew, M. G.; Hudson, M. J.; Iveson, P. B.; Russell, M. L.; Liljenzin, J.-O.; Skälberg, M.; Spjuth, L.; Madic, C. *J. Chem. Soc., Dalton Trans.* **1998**, 2973.

(25) Wu, J.; Watson, M.; Zhang, L.; Wang, Z.; Müllen, K. *J. Am. Chem. Soc.* **2004**, *126*, 177.

(26) Yu, X.-F.; Lu, S.; Ye, C.; Li, T.; Liu, T.; Liu, S.; Fan, Q.; Chen, E. Q.; Huang, V. *Macromolecules* **2006**, *39*, 1364.

(27) Sakamki, K.; Ohshita, J.; Kunai, A.; Nakao, H.; Adachi, H.; Okita, K. *Appl. Organomet. Chem.* **2001**, *15*, 604.

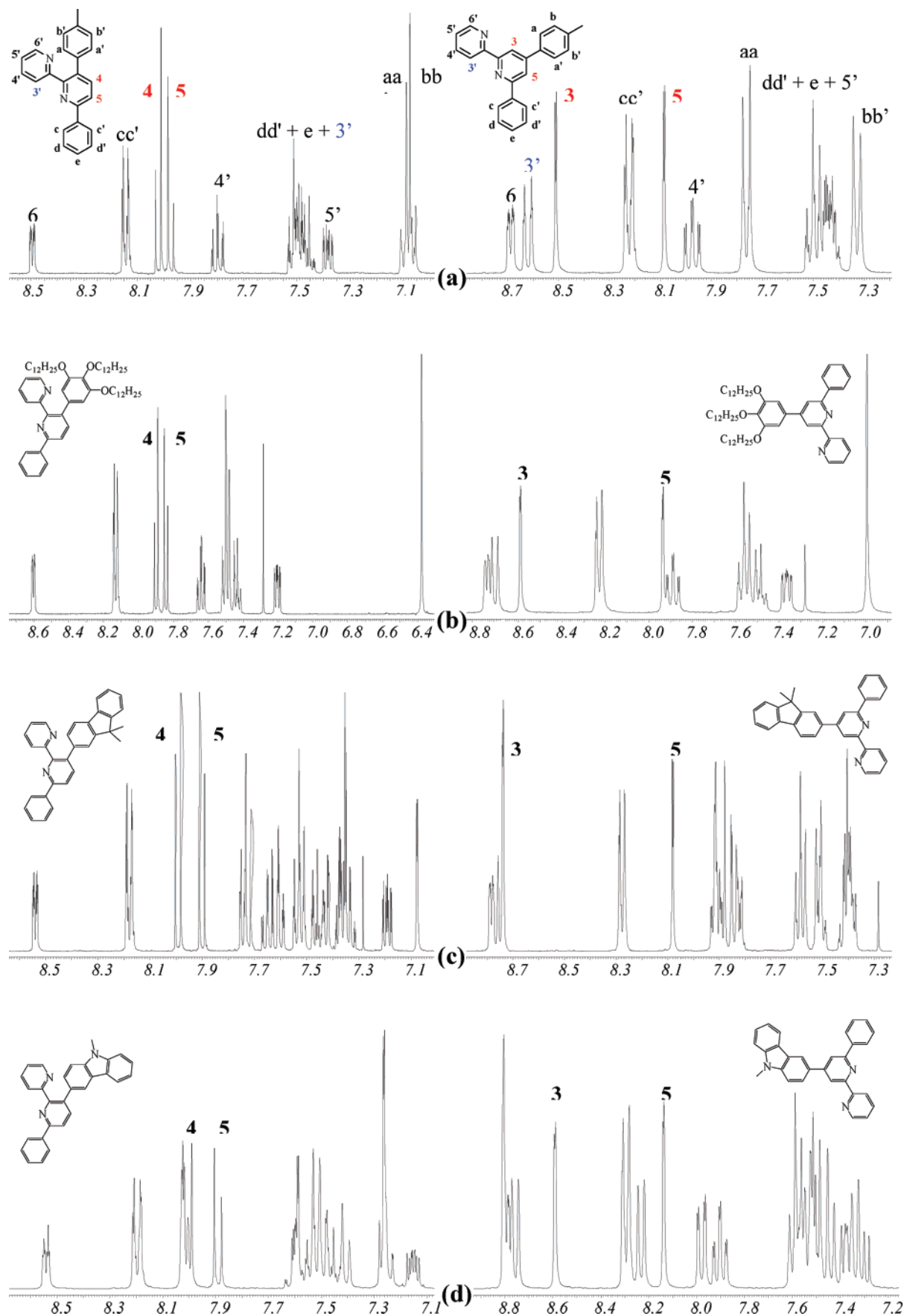


FIGURE 1. ^1H NMR spectra (aromatic resonances only) recorded in CD_3OD for (a) **2a** and **2b** and in CDCl_3 for (b) **3a** and **3b**, (c) **4a** and **4b**, and (d) **5a** and **5b**.

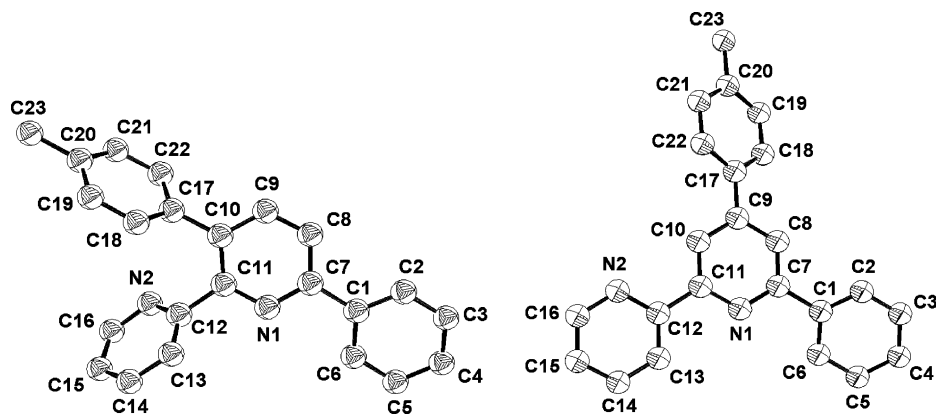
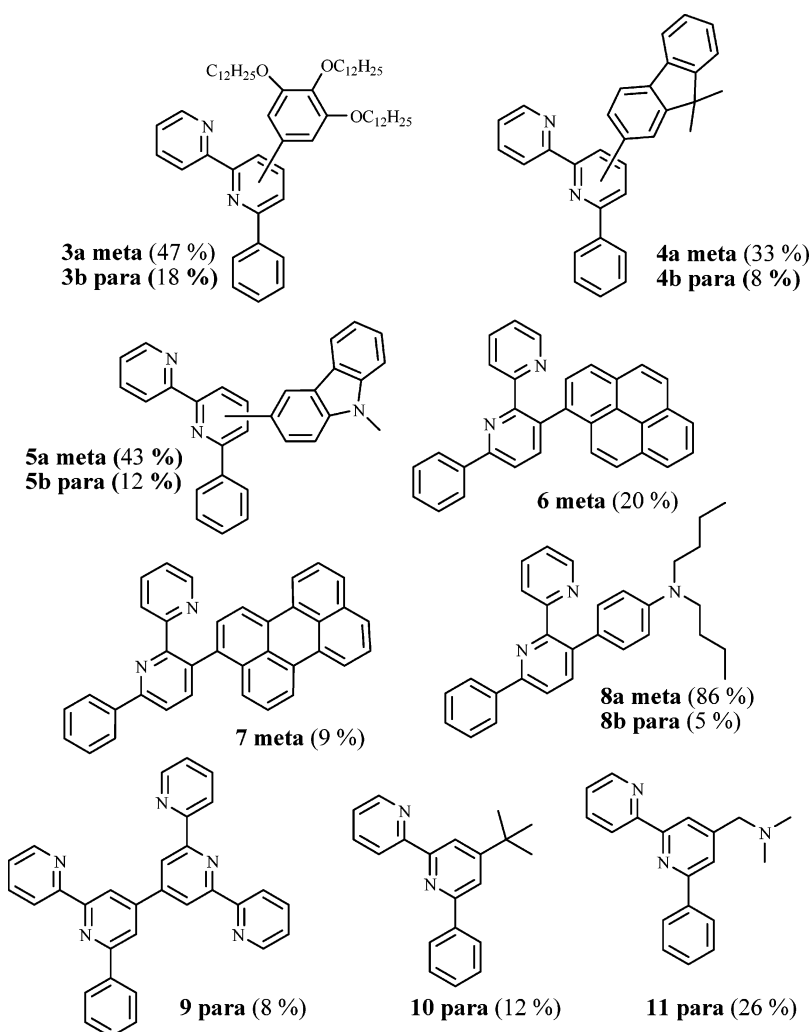


FIGURE 2. ORTEP view of compounds **2a** (left) and **2b** (right) (50% probability displacement ellipsoids), with all hydrogen atoms removed for the sake of clarity.

SCHEME 2



In terms of mechanism, we hypothesize that the meta isomer predominates due to favorable π – π interactions in the transition state between the ethynylaryl and the external pyridine rings (Figure 3). In the absence of such a stabilizing interaction, the para isomer should be favored for steric reasons. In keeping with such a hypothesis is the fact that the bulky 4-ethynyl-2,2':6',2''-terpyridine, and the nonaromatic 3,3'-dimethylbutyne and 1-dimethylamino-2-propyne substrates reacted with the triazine **1** to give exclusively the para isomers. This can be understood

assuming that the reaction partners adopt an orientation in the transition state that minimizes unfavorable steric interaction between the bulky terpyridine or *tert*-butyl fragment and the pyridine substituent. The absence of favorable aromatic interactions might also be in favor for the formation of the less encumbered para isomer.

Interestingly, 1-dimethylamino-2-propyne underwent smooth condensation to afford the para isomer **11** in acceptable yields (Scheme 2). This result can be attributed to the fact that this

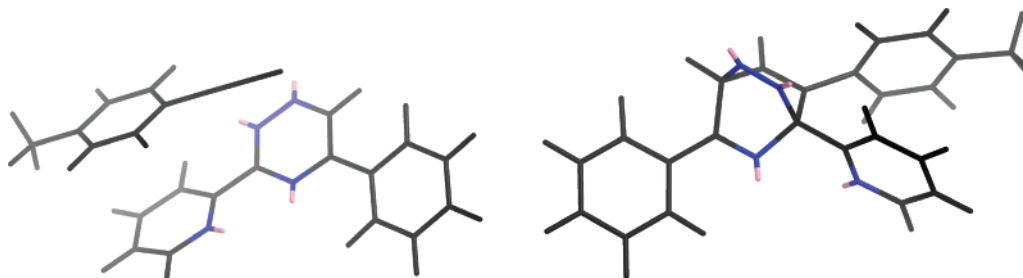
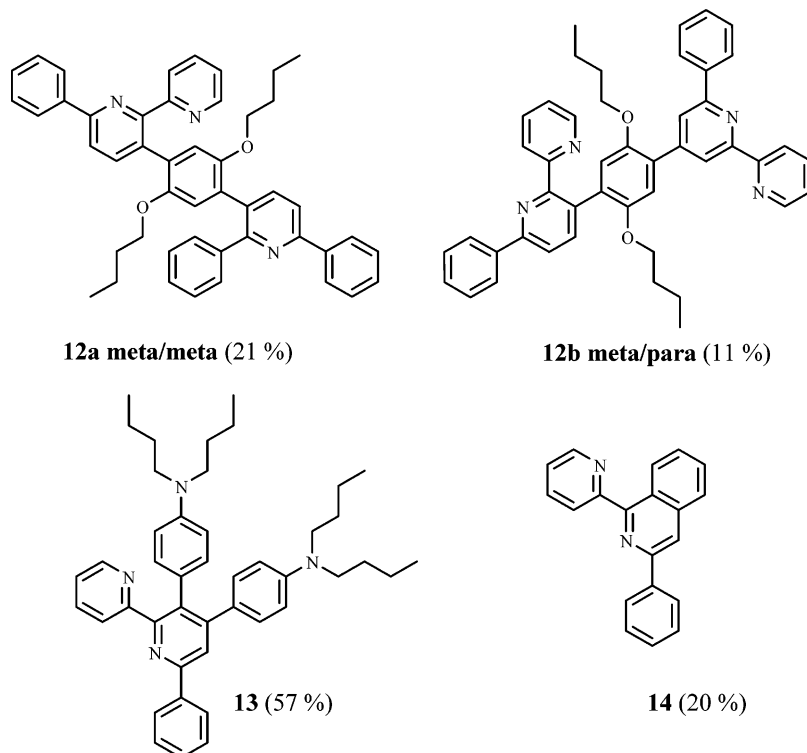


FIGURE 3. Schematic representation of (a) the bimolecular contact between the triazine and ethynyl derivative and (b) the transition state. (Representation obtained with energy minimization in Chem3D.)

SCHEME 3



stable and non-encumbered alkyne can easily approach the 2,5 positions of the triazine to induce the reverse-Diels–Alder condensation. Such regioselectivity has previously been observed with stannane derivatives.²¹

Subsequent work was focused on the use of soluble diacetylene derivatives, disubstituted acetylene derivatives, and benzyne in the retro-Diels–Alder reaction. The use of 1,4-diethynyl-2,5-dibutoxyphenyl³⁵ produced a mixture of two major isomers, the meta/meta derivative **12a** and the meta/para derivative **12b** (Scheme 3). The para/para compound was present in very low quantities and could not be thoroughly characterized. The condensation of 1,2-di(4-*N,N*-dibutylaminophenyl)ethyne³⁶ with 6-phenyl-2-pyridyl-1,3,4-triazine produced ligand **13** in 57% yield. A similar reaction of benzyne prepared in situ from anthranilic acid and isoamyl nitrite³⁷ gave compound **14** in 20% isolated yield.

The molecular structure of **13** was established by single-crystal X-ray diffraction (Figure 4). As in compounds **2a** and

2b, the nitrogen atoms of the bipyridine moiety of **13** lie in a transoid position, although the bipyridine unit is far from planar,

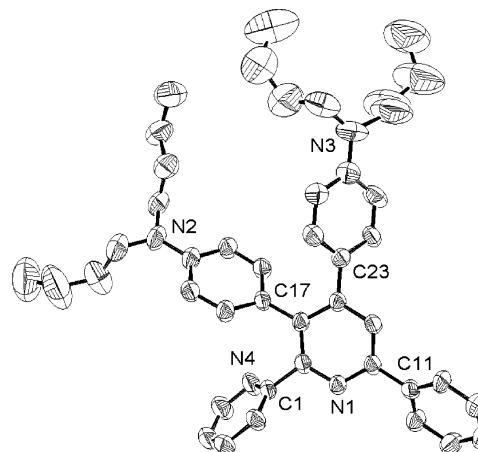
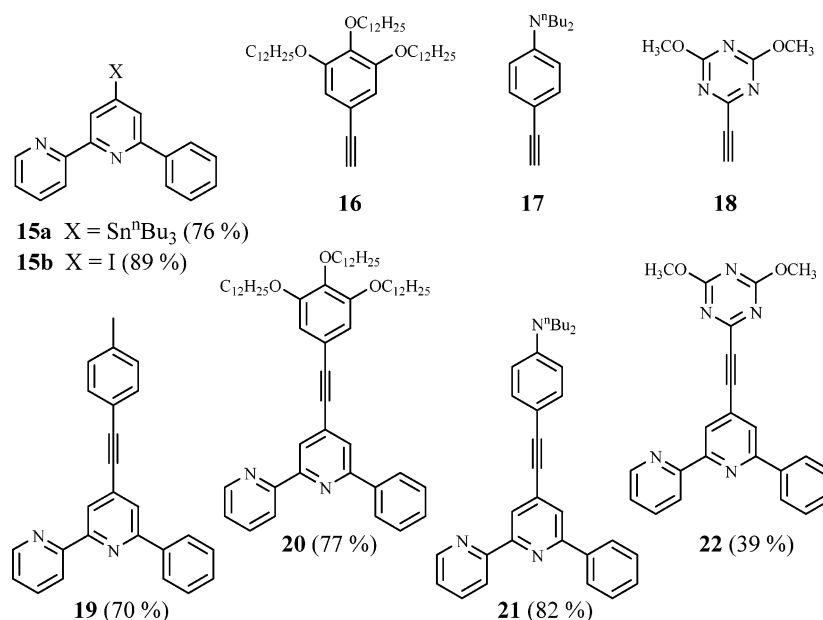


FIGURE 4. ORTEP view of compound **13** (30% probability displacement ellipsoids), with all hydrogen atoms removed for the sake of clarity.

(35) Ziessel, R.; Diring, S.; Retaillieu, P. *Dalton Trans.* **2006**, 3285.

(36) Umezawa, H.; Okada, S.; Oikawa, S.; Matsuda, H.; Nakanishi, H. *J. Phys. Org. Chem.* **2005**, 18, 468.

SCHEME 4



with a ring dihedral angle of 66.4°. This is presumably a consequence of the proximity of a dibutylaminophenyl substituent on the tetrafunctionalized pyridine to the simple pyridine substituent. The phenyl ring is also strongly tilted (dihedral angle 38.8°) with respect to the pyridine ring, this facilitating aromatic–aromatic ($\text{CH}\cdots\pi$) interactions with both a tolyl group (at 1 $-x$, $-y$, 2 $-z$) and a pyridine ring (at x , $\frac{1}{2} - y$, $\frac{1}{2} + z$) of adjacent molecules. Tilting of both dibutylaminophenyl rings with respect to the pyridine (dihedral angles of 49.6 (meta) and 48.7° (para)) is associated with aggregation of the butyl chains within the lattice.

Condensation of the triazine **1** with tri-*n*-butyl(ethynyl)tin provides compound **15a** in 76% yield. Conversion of the stannane derivative **15a** to the iodo derivative **15b** is straightforward by reaction with iodine in chloroform (89%). **15b** is a valuable intermediate for the preparation of various ethynyl-substituted platforms such as **16**, **17**, and **18**. By employing a standard protocol ([Pd(PPh₃)₂Cl₂] 6 mol % and CuI 10 mol %) at rt, the stable cross-coupled compounds **19** to **22** (Scheme 4) were isolated in acceptable yields (70%, 77%, 82%, and 39%, respectively).

Unfortunately, attempts to complex ligand **20** with [Pt-(DMSO)₂Cl₂]³⁸ or K₂PtCl₄ in water/acetonitrile or water/THF were unsuccessful and achieved only in very low yield for **19**. This unfavorable result is likely due to the inductive electron-donating character of the ethynyl residue,³⁹ rendering the phenyl groups less acidic and more difficult to deprotonate by ortho-metallation to the aromatic residue. Fortunately, the iodo-containing ligand **15b** afforded the desired complex **23** by complexation with K₂PtCl₄ in water/acetonitrile despite our concern that the aryl-iodo fragment might promote competitive side reactions (Scheme 5). With this pivotal complex **23** in hand, we were pleased to find it possible to selectively substitute the platinum-chloro ligand by ethynyltolyl and the ethynyl derivative

16, leading respectively to the stable complexes **24** and **25** in respectable yields (Scheme 5). This reaction took place smoothly in the presence of CuI (6 mol %) at rt under anaerobic conditions by using triethylamine to quench the nascent acid. In a further demonstration of the versatility of these procedures, the iodo group was found to be easily substituted by the ethynyl derivative **16** under Sonogashira conditions, providing the highly functionalized and unsymmetrically substituted platinum complex **27**. As well, simultaneous cross-coupling of both the iodo and chloro groups could be performed by using [Pd(PPh₃)₄] and ethynyltoluene (2 equiv) under anaerobic conditions and in the absence of Cu(I), leading to the symmetrically substituted derivative **26**.

To characterize ligand **15b** in its bound form and to establish various substituent orientations in these Pt(II) complexes, single-crystal structure determinations were performed on compounds **23** and **24** (Figure 5).

These studies revealed a distorted square-planar geometry of the Pt^{II} center, with the tridentate ligand *quasi*-planar in all cases.⁴⁰ The Pt–C bond lengths are not unusual, although that in **23** is significantly longer than those of **24**. The platinum–nitrogen bond lengths trans to the phenyl group (2.062–2.131 Å) are markedly longer than those trans to the chlorine or the ethynyltoluyl ligands (1.941–1.966 Å). In the Pt-ethynyl-tolyl derivative structure **24**, the tolyl group is tilted out of the plane of the Pt core by 76.3° but is *quasi*-parallel to the *bc* plane of the unit cell, whereas the N2–Pt–C17/C18–C19 axe lie parallel to the plane (1, 0, –1), with an aromatic ring plane separation of ~3.4 Å being indicative of π – π stacking.

Optical Properties. The absorption spectra (Figure 6) display several well-resolved absorption bands in the 230–420 nm range attributed to π – π^* transitions of the phenyl and pyridine rings and n – π transitions due to the presence of heteroatoms in the framework.^{41,42} In the carbazole cases **5a/b** the low-energy absorption bands are bathochromically shifted by 22 nm with

(37) Gonsalves, A.; Pinho e Melo, T.; Gilchrist, T. *Tetrahedron* **1992**, 48, 6821.

(38) Price, J. H.; Birk, J. P.; Wayland, B. B. *Inorg. Chem.* **1978**, *17*, 2245.

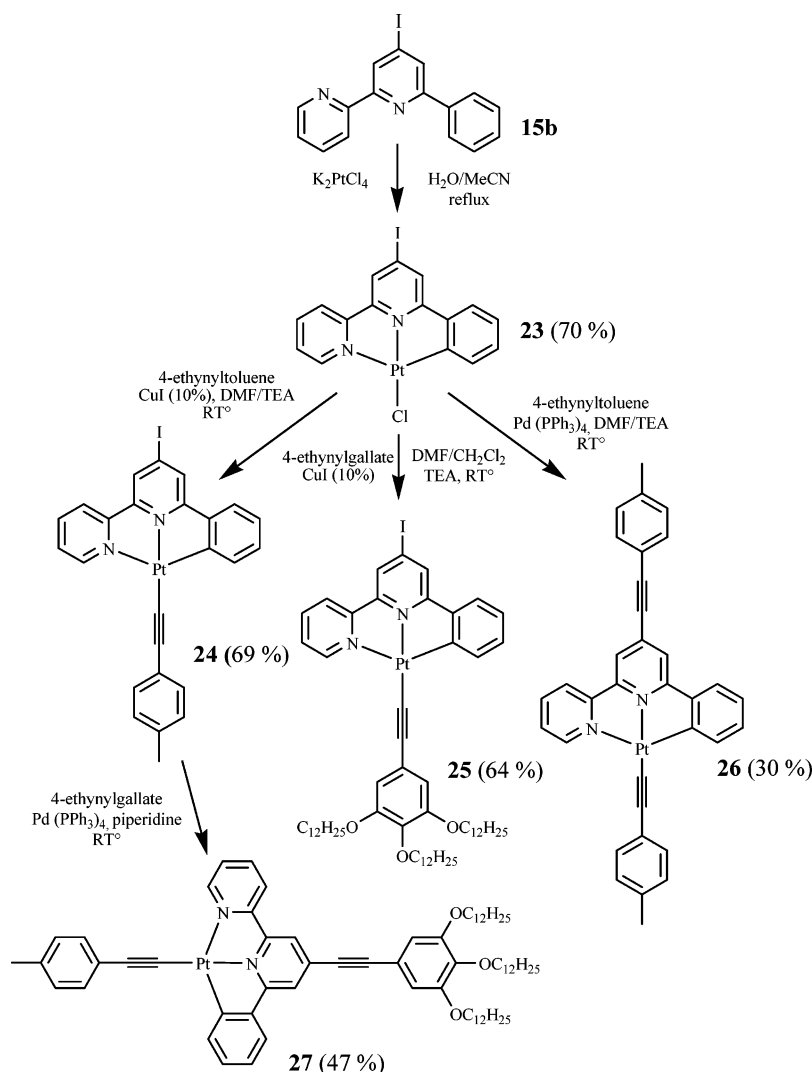
(39) Pohl, R.; Anzenbacher, P. *Org. Lett.* **2003**, *5*, 2769.

(40) Lu, W.; Mi, B. X.; Chan, M. C. W.; Hui, Z.; Zhu, N. Y.; Lee, S. T.; Che, C. M. *Chem. Commun.* **2002**, 206.

(41) Melhuish, W. H. *J. Phys. Chem.* **1961**, 65, 229.

(42) Meech, S. R.; Phillips, D. J. *Photochem.* **1983**, 23, 193.

SCHEME 5



respect to the fluorene molecules **4a/b** (Table 1). This shift to low energy is enhanced when a triple bond is present in the para position of the dibutylaminophenyl-substituted compounds (compare compounds **21** and **8b**, Figure 6b). This effect reflects a better delocalization in the ground state between the acceptor fragment (bipyridine subunit) and the electron-donating fragments such as *N*-methylcarbazole and *N,N*-dibutylaminophenyl. This delocalization is clearly hindered when the carbazole or phenyl rings are directly linked to the central pyridine ring in the meta and para regioisomers due to steric effects responsible for the twist of the phenyl ring with respect to the mean plane (see X-ray structures in Figures 2 and 4). No particular absorption differences are observed between the meta and the para isomers within the same series. Note that when two dibutylamino groups are present in compound **13**, a 20 nm hypsochromic shift is observed (Figure 6b), possibly due to the destabilization of the $S_0 \rightarrow S_1$ transition. In the isoquinoline compounds **14** two absorption bands at 311 and 242 nm are clearly evident, in keeping with previous data obtained on similar ligands.⁴³

Most of these novel ligands are luminescent in solution at *rt* with fluorescence maxima progressively shifted to lower energy

for the meta versus the para isomers (Figure 7 and Table 1). This is a general trend, the meta regioisomer always fluoresces at lower energy than the para regioisomer and the latter always exhibits a much higher fluorescence quantum yield versus the meta. For instance, in the tolyl case **2b** (para isomer) the quantum yield reaches 38% whereas the meta case **2a** is not fluorescent at all. The excitation spectra measured at the lower emission band match perfectly the absorption spectra, meaning in each case that the fluorescence originates from a single excited state (Figure 7).

With the exception of the pyrene and perylene cases, the fluorescence spectra show very poor mirror symmetry with the lowest energy absorption band and they indeed look very different. For all the compounds, the emission spectra are similar in shape and significantly red-shifted compared to the absorption spectra, indicating a strong Stokes shift, which suggests a reorganization occurring in the excited state (Table 1). The presence of a triplet excited state is excluded on the basis of the absence of any oxygen effect in the steady-state emission and quantum yields. The very short excited state lifetimes that were measured in some cases (*vide infra*) are in keeping with such a statement.³⁷ In fact, the broad and structureless absorption bands are reminiscent of charge transfer (CT) transitions and it is noteworthy that these ligands contain electron-donating groups

(43) Anton, M. F.; Moomaw, W. R. *J. Chem. Phys.* **1977**, 66, 1808.

(44) Olmsted, J. J. *Phys. Chem.* **1979**, 83, 2581.

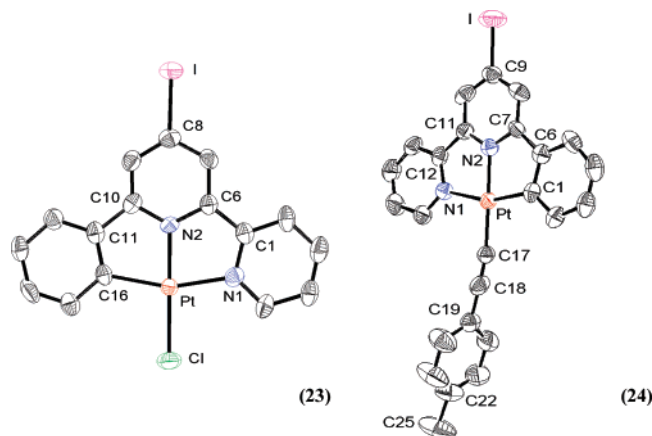


FIGURE 5. ORTEP view of compounds **23** and **24** (50% probability displacement ellipsoids), with all hydrogen atoms removed for the sake of clarity. Selected distances (Å) and angles (deg) for **23**: Pt–N(1) 1.941, Pt–N(2) 2.062, Pt–C(16) 2.088, Pt–Cl 2.304, N(1)–Pt–N(2) 80.89, N(1)–Pt–C(16) 160.65, N(2)–Pt–Cl 179.15. Selected distances (Å) and angles (deg) for **24**: Pt–N(1) 2.093, Pt–N(2) 1.980, Pt–C(1) 1.983, Pt–C(17) 1.985, C(17)–C(18) 1.182, N(1)–Pt–N(2) 79.02, N(1)–Pt–C(1) 160.83, N(2)–Pt–C(17) 175.75.

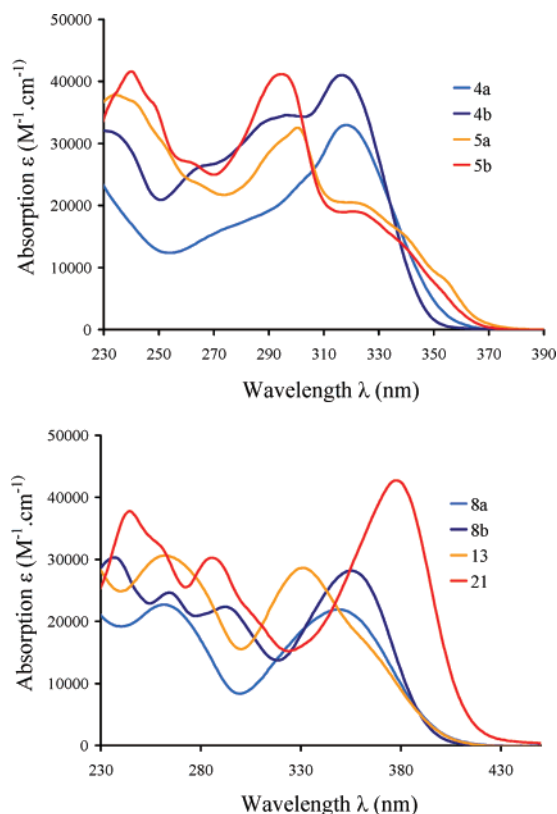


FIGURE 6. Absorption spectra of (a) **4a**, **4b**, **5a**, and **5b** and (b) **8a**, **8b**, **13**, and **21** measured in CH_2Cl_2 at rt, at ca. $3 \cdot 10^{-5}$ M.

(the alkyl and alkoxy chain, the tertiary amines, ...) and electron-accepting fragments such as the bipyridine and the acetylenic subunits. The latter groups promote charge transfer along the molecular axis.^{45,46} The large Stokes shifts of 1000 to 10000 cm^{-1} are in keeping with a CT state and not a pure π – π^*

TABLE 1. Spectroscopic Data for the Compounds at 298 K^a

compd	λ_{abs} (nm)	ϵ ($\text{M}^{-1}\text{cm}^{-1}$)	λ_{F} (nm)	Stokes' shift (cm^{-1})	fwhm (cm^{-1}) ^b	Φ_{F} ^c
2a	289	22900				
2b	264	43300	362	4427	3333	38
3a	306	21000	451	10507	4156	4.1
3b	285	29500	435	9584	4476	34.6
4a	318	33000	410	7056	4551	1.7
4b	318	41000	372	4564	3580	66
5a	319	20500	438	8516	4507	4.7
5b	320	19000	402	6374	3308	53
6	349	40100	417	4672	3732	1.5
7	450	34500	470	945	2196	37
8a	350	21900	487	8037	3644	7.4
8b	356	28200	461	6397	3443	31.1
9	315	15100	374	5008	3285	17
10	283	15000	346	4101	3869	3.5
11	304 sh	10600	358	4961	3890	1.8
12a	338 sh	17600	422	5889	3701	<1
12b	328 sh	18500	424	6902	3339	5.9
13	332	28600	468	8752	3492	<1
14	312	7400	429	8741	4481	5.5
19	310	33000	357	4246	3234	41.5
20	323	31000	440	8232	3905	43
21	378	42700	480	5621	3326	28.4
22	332	7900	391	4545	3427	19

^a Determined in dichloromethane solution. ^b fwhm measurements. ^c Determined in aerated dichloromethane solution (ca 10^{-6} M) with quinine bisulfate dihydrate in 0.5 M H_2SO_4 solution as standard, which absorbs at 366 nm and emits at 456 nm with a known quantum yield of $\Phi_{\text{F}} = 0.546$.⁴³ All Φ_{F} are corrected for changes in refractive index.

emitting state. The involvement of CT states is further confirmed by studying the influence of solvent (Figure S2, Supporting Information).

For the pyrene, perylene, and quinoline cases, the situation looks quite different (Figure 8). The fluorescence spectrum shows excellent mirror symmetry with the lowest energy absorption and, in fact, this is confirmed by excitation spectra obtained under similar experimental conditions. On this basis, we assign the absorption and fluorescence peaks to spin-allowed π , π^* transitions. The lowest energy singlet state $S_0 \rightarrow S_1$ is responsible for this intense fluorescence emission band without any perturbation of a CT state. In fact, the fluorescence of compounds **6**, **7**, and **14** is dominated by the emission of the pyrene, perylene, and isoquinoline fragments.

As would be expected from singlet excited states mixed with some charge-transfer character, the excited state lifetimes lie within the nanosecond time scale. Indeed, the fluorescence decay profiles could be described by a single-exponential fit, with fluorescence lifetimes in the range of 1 to 10 ns, in accordance with a singlet excited state (Table 2). In fact, most of the radiative rate constants lie within the 3 to $6 \times 10^{-7} \text{ s}^{-1}$ range (Table 2). However, the nonradiative rate constants are significantly higher than the radiative rate constants, mostly because of the short excited state lifetime, which may be attributed to the interaction of the emitting state with an energetically low-lying localized state. At this stage of our investigation, we do not have evidence for the formation of a triplet excited state that could quench the fluorescence.

Electrochemical data for the di-*n*-butylamino grafted molecules, derived from cyclic voltammetry in dichloromethane, are gathered in Table 2. The prototypical *p*-toluyl molecules **2a** and **2b** are inactive within the electrochemical window used (+1.8 V to –2.2 V versus SCE). As expected, ligands **8a**, **8b**, and **21** display a reversible oxidation wave around +0.8 V, results in keeping with the oxidation of $^n\text{Bu}_3\text{N}$ occurring at

(45) Harriman, A.; Rostron, S. A.; Khatyr, A.; Ziessel, R. *Faraday Discuss.* **2006**, *131*, 377.

(46) Khatyr, A.; Ziessel, R. *J. Org. Chem.* **2000**, *65*, 7814.

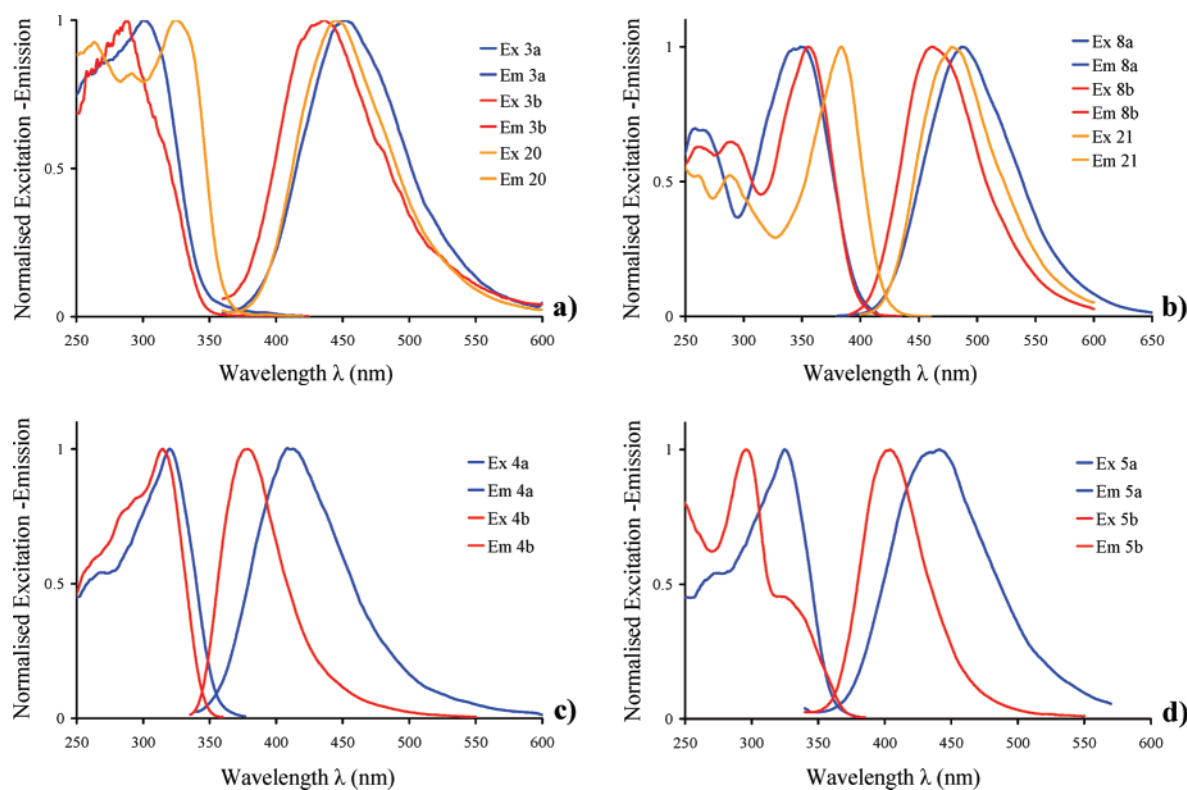


FIGURE 7. Normalized emission and excitation spectra measured in CH_2Cl_2 at rt: (a) **3a**, **3b**, and **20**, (b) **8a**, **8b**, and **21**, (c) **4a** and **4b**, and (d) **5a** and **5b**.

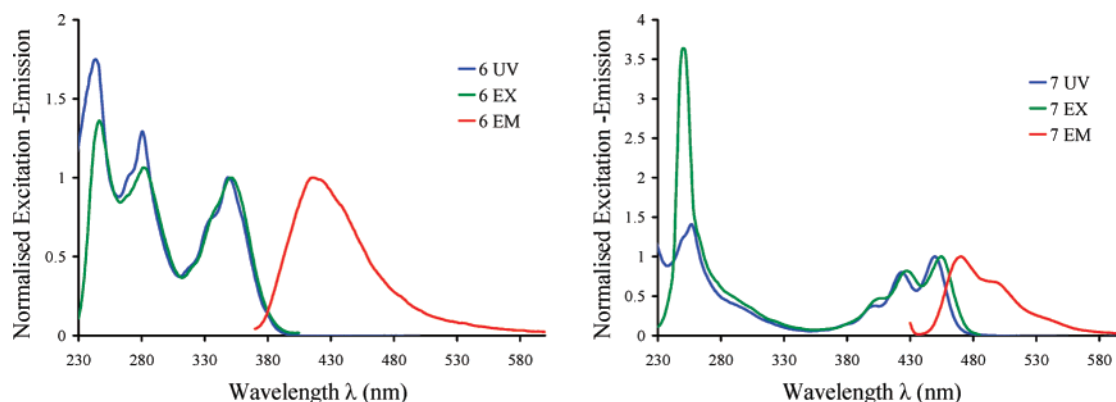


FIGURE 8. Normalized absorption (blue), excitation (green), and emission (red) spectra in CH_2Cl_2 of **6** (left) and **7** (right).

TABLE 2. Spectroscopic Data in Dichloromethane Solution at 298 K

comps	λ_{abs} (nm)	ϵ ($\text{M}^{-1} \text{cm}^{-1}$)	λ_{F} (nm)	Φ_{F}^a (%)	τ_{F} (ns)	k_{r}^b (10^8s^{-1})	k_{nr}^b (10^8s^{-1})	ΔG_{ES}^c (eV)	$E^\circ(\text{L}^{+\bullet}/\text{L})$ (V) (ΔE_{p} (mV) ^d)	$E^\circ(\text{L}^{+\bullet}/\text{L}^*)$ (eV) ^e
8a	350	21,900	487	7.4	2.6	28.5	3.6	2.92	+ 0.73 (70)	−2.19
8b	356	28,200	461	31.1	6.3	49.4	1.1	3.00	+ 0.83 (60)	−2.17
21	378	42,700	480	28.4	4.7	60.4	1.5	2.91	+ 0.79 (75)	−2.12

^a Determined in degassed dichloromethane solution (ca. 10^{-6} M) with quinine bisulfate dihydrate in 0.5 M H_2SO_4 solution as standard, which absorbs at 347 nm and emits at 448 nm with a known quantum yield of $\Phi_{\text{F}} = 0.546$.⁴⁴ All Φ_{F} are corrected for changes in refractive index. ^b Calculated by using the following equations: $k_{\text{r}} = \Phi_{\text{F}}/\tau_{\text{F}}$, $k_{\text{nr}} = (1 - \Phi_{\text{F}})/\tau_{\text{F}}$, assuming that the emitting state is produced with unit quantum efficiency. ^c Excited state energies were estimated ($\pm 5\%$) by drawing a tangent on the high-energy side of the emission; λ (nm) $\times E$ (eV) = 1239.8. ^d Potentials determined by cyclic voltammetry in deoxygenated CH_2Cl_2 solution, containing 0.1 M TBAPF₆, at a solute concentration of ca. 1 mM and at 20 °C. Potentials were standardized versus ferrocene (Fc) as internal reference and converted to the SCE scale assuming that $E_{1/2}(\text{Fc}/\text{Fc}^+) = +0.38$ V ($\Delta E_{\text{p}} = 70$ mV) vs SCE. The error in half-wave potentials is ± 10 mV. ^e Calculated excited state oxidation potential vs SCE, $E^\circ(\text{L}^{+\bullet}/\text{L}^*) = E^\circ(\text{L}^{+\bullet}/\text{L}) - \Delta G_{\text{ES}}$. L accounts for the ligands

+0.69 V versus SCE.⁴⁷ Note that di-*n*-butylamino derivatives are more difficult to oxidize by 100 mV compared to the tertiary amine. The meta regioisomer **8a** is easier to oxidize than the para isomer by 100 mV likely due to a better stabilization of

the radical cation generated after single electron oxidation. Unlike certain oligopyridine adducts,⁴⁸ there is no indication of the reduction of the bipyridine-phenyl fragment within the given electrochemical window.

As all excited state energies lie in the 2.91–3.00 eV range, calculation of the redox potential of the first excited states from the measured oxidation potentials enables the conclusion to be drawn that these excited states are strong reductants (Table 2).

Concluding Remarks

An interesting facet of this chemistry is the fact that various highly functionalized polypyridine ligands suitable for transition metal complexation can be easily prepared. The reverse Diels–Alder reaction, effective with various ethynyl-substituted derivatives, is regioselective when sterically hindered ethynyl substrates are transformed. The introduction of functionalized ethynyl groups opens the way to a new class of C^NN-tridentate ligands bearing various functionalities, some of which include solubilizing chains, additional chromophoric residues, and easily transformable functions. This methodology accommodates various functional groups and affords the anticipated substituted aromatics in good to excellent yields. Unfortunately, the ligands bearing ethynyl-substituted groups attached to the central pyridine ring do not provide platinum complexes. Fortunately, with the iodo function present on the ligand, platinum complexation and cross-coupling with various ethynyl-grafted residues is feasible and allows the introduction of different functional groups on the central pyridine ring. Of particular interest is the (iodo-ligand)–Pt–Cl complex for which orthogonal substitution of the iodo or the chloro substituent can be achieved by using the appropriate catalysts. In particular, it can be used in the synthesis of hybrid complexes bearing the donor or the acceptor at a predetermined position. The resulting ligands display intriguing optical properties such as strong absorption in the visible and strong fluorescence at rt due to a mixed emissive state with a pronounced charge-transfer character. The use of these ligands to synthesize multimetallic complexes pre-organized at different places and carrying various redox and optical properties is currently in progress in our laboratory.

Experimental Section

General Procedure 1 for the Diels–Alder Reaction. A Schlenk tube was charged with 6-phenyl-2-pyridyl-1,3,4-triazine **1**, the appropriate ethynyl compound, and *o*-dichlorobenzene. The mixture was argon-degassed via at least three freeze–pump–thaw cycles, heated to 180 °C, and finally stirred in the dark for 1 to 3 days. The solvent was removed under high vacuum. The residue was treated with water and extracted with dichloromethane. The organic extracts were washed with water, then with saturated brine and filtered through cotton wool. The solvent was removed by rotary evaporation and the residue was purified by column chromatography.

General Procedure 2 for the Sonogashira Cross-Coupling Reaction. A Schlenk flask was charged with 4-iodo-6-phenyl-2,2'-bipyridine, the appropriate ethynyl derivative, [Pd(PPh₃)₂Cl₂] (10% mol), tetrahydrofuran, and diisopropylamine (v/v, 7/1), except for **22** where triethylamine was used. The mixture was argon-degassed for 30 min, then CuI (10 mol %) was introduced and the reaction mixture stirred at room temperature for 18 h. The solvent was evaporated, and the residue was treated with water and extracted with dichloromethane. The organic extracts were washed with water, then with saturated brine and filtered through hygroscopic cotton wool. After rotary evaporation, the residue was purified by column chromatography.

General Procedure 3 for the Preparation of Platinum Complexes. The appropriate 6-phenyl-2,2'-bipyridine ligand and K₂PtCl₄ were dissolved in a mixture of acetonitrile–water (v/v 2/1). The mixture was refluxed for 18 to 24 h. The resulting orange precipitate was centrifuged and successively washed with water, acetonitrile, and diethyl ether. Single crystals for X-ray diffraction were obtained by vapor diffusion of diethyl ether in a dimethyl sulfoxide solution containing the chloroplatinum complex.

General Procedure 4 for the Copper-Promoted Coupling Reaction. The chloroplatinum complex and the ethynyl derivative were dissolved in the appropriate solvent (either CH₂Cl₂, DMF, or CH₂Cl₂/DMF). Triethylamine was added and the mixture was degassed by bubbling argon for 30 min, after which CuI was added and the reaction mixture was stirred in the dark at room temperature for 1 to 3 days. The residue was treated with water and extracted with dichloromethane. The organic extracts were washed with water, then with saturated brine and filtered through hygroscopic cotton wool. The solvent was removed by rotary evaporation and the residue was purified by column chromatography.

3-(*p*-Tolyl)-6-phenyl-2,2'-bipyridine (2a): prepared, using procedure 1, from 6-phenyl-2-pyridyl-1,3,4-triazine **1** (300 mg, 1.28 mmol), *p*-tolylacetylene (330 μ L, 2.70 mmol), and 1,2-dichlorobenzene (1 mL); chromatography on silica gel eluting with petroleum ether to dichloromethane to give 173 mg (42%) of **2a** as a white solid after precipitation in pentane; ¹H NMR (CD₃OD, 300 MHz) δ 8.47 (ddd, 1H, *J* = 4.9 Hz, 1.7 Hz, 0.9 Hz), 8.14–8.11 (m, 2H), 7.98 (ABsys, 2H, *J*_{AB} = 8.1 Hz, *v*₀ δ = 12.7 Hz), 7.78 (td, 1H, ³*J* = 7.7 Hz, ⁴*J* = 1.8 Hz), 7.52–7.40 (m, 4H), 7.36 (ddd, 1H, *J* = 7.6 Hz, 5.0 Hz, 1.2 Hz), 7.10–7.03 (m, 4H), 2.30 (s, 3H); ¹³C NMR (CDCl₃, 75 MHz) δ 158.9, 155.7, 155.6, 148.9, 139.4, 139.0, 136.7, 136.6, 136.0, 135.0, 129.2, 128.9, 128.7, 127.1, 124.9, 122.4, 119.8, 21.2; UV–vis (CH₂Cl₂) λ (nm) (ϵ , M^{−1} cm^{−1}) 288 (22800), 277 (22800); IR (KBr, cm^{−1}) ν 3053 (w), 3024 (w), 2915 (w), 2854 (w), 1580 (m), 1565 (s), 1452 (s), 1423 (s), 1207 (w), 1092 (m), 804 (s), 756 (s); FAB⁺ *m/z* (nature of the peak, rel intensity) 323.1 ([M + H]⁺, 100). Anal. Calcd for C₂₃H₁₈N₂: C, 85.68; H, 5.63; N, 8.69. Found: C, 85.52; H, 5.32; N, 8.40.

4-(*p*-Tolyl)-6-phenyl-2,2'-bipyridine (2b): 55 mg (13%) of **2b** as a white solid after precipitation in pentane; ¹H NMR (CD₃OD, 300 MHz) δ 8.69–8.66 (m, 1H), 8.61 (dt, 1H, ³*J* = 8.0 Hz, 1.0 Hz), 8.50 (d, 1H, ⁴*J* = 1.5 Hz), 8.24–8.20 (m, 2H), 8.09 (d, 1H, ⁴*J* = 1.5 Hz), 7.98 (td, 1H, ³*J* = 7.7 Hz, ⁴*J* = 1.8 Hz), 7.78 (d, 2H, ³*J* = 8.3 Hz), 7.56–7.43 (m, 4H), 7.36 (d, 2H, ³*J* = 7.9 Hz), 2.42 (s, 3H); ¹³C NMR (CDCl₃, 75 MHz) δ 157.1, 156.5, 156.2, 150.1, 149.1, 139.6, 139.1, 136.8, 135.8, 129.7, 129.0, 128.8, 127.1, 123.8, 121.5, 118.3, 117.3, 21.3; UV–vis (CH₂Cl₂) λ (nm) (ϵ , M^{−1} cm^{−1}) 311 (9500), 278 sh (37500), 264 (43300); IR (KBr, cm^{−1}) ν 3034 (w), 2920 (w), 1598 (m), 1565 (s), 1470 (m), 1387 (s), 816 (s), 768 (s); FAB⁺ *m/z* (nature of the peak, rel intensity) 323.1 ([M + H]⁺, 100). Anal. Calcd for C₂₃H₁₈N₂: C, 85.68; H, 5.63; N, 8.69. Found: C, 85.47; H, 5.47; N, 8.52.

3-(Perylen-3-yl)-6-phenyl-2,2'-bipyridine (7): prepared, using procedure 1, from 5-phenyl-3-(2-pyridyl)-1,3,4-triazine (85 mg, 0.36 mmol), 3-ethynylperylene (100 mg, 0.36 mmol), and 1,2-dichlorobenzene (1 mL); chromatography on alumina eluting with dichloromethane–petroleum ether (v/v 25/75 to 50/50), second chromatography on silica gel eluting with dichloromethane to give 15 mg (9%) of **7** as an orange to brown powder; ¹H NMR (CDCl₃, 400 MHz) δ 8.33–8.31 (m, 1H), 8.22–8.13 (m, 6H), 7.92 (ABsys, 2H, *J*_{AB} = 8.0 Hz, *v*₀ δ = 6.8 Hz), 7.69 (d, 2H, ³*J* = 8.0 Hz), 7.6 (d, 1H, ³*J* = 8.0 Hz), 7.55–7.44 (m, 7H), 7.34–7.29 (m, 2H), 6.99 (ddd, 1H, *J* = 7.5 Hz, 5.0 Hz, 1.0 Hz); ¹³C NMR (CDCl₃, 100 MHz) δ 158.2, 156.6, 156.5, 149.0, 140.8, 139.1, 137.7, 135.9, 134.9, 133.7, 133.1, 131.5, 131.4, 131.3, 130.9, 129.3, 128.9, 128.7, 128.6, 128.0, 127.3, 126.8, 126.7, 125.9, 124.3, 122.5, 120.5, 120.4, 120.0, 119.7; UV–vis (CH₂Cl₂) λ (nm) (ϵ , M^{−1} cm^{−1}) 450 (34500), 423 (27000), 401 (13000), 293 sh (13100), 257 (48500); IR (KBr, cm^{−1}) ν 3049 (w), 1585 (m), 1563 (m), 1461 (m), 1420 (m), 1386 (m), 810 (s), 748 (s); FAB⁺ *m/z* (nature of the peak, rel intensity)

(47) Mann, C. K. *Anal. Chem.* **1961**, 36, 2424.

(48) Goeb, S.; De Nicola, A.; Ziessel, R. *J. Org. Chem.* **2005**, 70, 1518.

483.1 ($[M + H]^+$, 100). Anal. Calcd for $C_{36}H_{22}N_2$: C, 89.60; H, 4.60; N, 5.81. Found: C, 89.47; H, 4.38; N, 5.59.

4-(*tert*-Butyl)-6-phenyl-2,2'-bipyridine (10): prepared, using procedure 1, from 5-phenyl-3-(2-pyridyl)-1,3,4-triazine (200 mg, 0.85 mmol), 3,3-dimethylbut-1-yne (315 μ L, 2.55 mmol), and 1,2-dichlorobenzene (1 mL); chromatography on silica gel eluting with dichloromethane to give 30 mg (12%) of **10** as a white solid; 1H NMR ($CDCl_3$, 400 MHz) δ 8.72–8.70 (m, 1H), 8.65 (d, 1H, $^3J = 8.0$ Hz), 8.44 (d, 1H, $^4J = 2.0$ Hz), 8.15 (d, 2H, $^3J = 7.0$ Hz), 7.83 (td, 1H, $^3J = 7.6$ Hz, $^4J = 1.7$ Hz), 7.78 (d, 1H, $^4J = 2.0$ Hz), 7.54–7.42 (m, 3H), 7.31 (ddd, 1H, $J = 7.4$ Hz, 4.9 Hz, 1.1 Hz), 1.46 (s, 9H); ^{13}C NMR ($CDCl_3$, 100 MHz) δ 161.9, 156.9, 156.8, 155.8, 149.1, 140.1, 136.9, 128.9, 128.8, 127.2, 123.7, 121.7, 117.8, 116.6, 35.4, 30.9; UV–vis (CH_2Cl_2) λ (nm) (ϵ , $M^{-1} cm^{-1}$) 306 sh (11000), 283 (14900), 260 (19000), 248 sh (22000), 241 (23500); IR (KBr, cm^{-1}) ν 3064 (w), 2960 (m), 2867 (w), 1600 (m), 1583 (m), 1542 (m), 1400 (m), 1247 (m), 1026 (m), 875 (m), 773 (s), 694 (s); FAB $^+$ m/z (nature of the peak, rel intensity) 289.1 ($[M + H]^+$, 100). Anal. Calcd for $C_{20}H_{20}N_2$: C, 83.30; H, 6.99; N, 9.71. Found: C, 82.99; H, 6.47; N, 9.52.

4-(*N,N*-Dimethylaminomethyl)-6-phenyl-2,2'-bipyridine (11): prepared, using procedure 1, from 5-phenyl-3-(2-pyridyl)-1,3,4-triazine (200 mg, 0.85 mmol), *N,N*-dimethylprop-2-yn-1-amine (200 μ L, 1.85 mmol), and 1,2-dichlorobenzene (1 mL); chromatography on aluminum oxide eluting with dichloromethane–petroleum ether (v/v 50/50 to 75/25) to give 64 mg (26%) of **11** as a light yellow solid; 1H NMR ($CDCl_3$, 400 MHz) δ 8.69 (dt, 1H, $J = 4.0$ Hz, 1.0 Hz), 8.65 (d, 1H, $^3J = 8.0$ Hz), 8.30 (s, 1H), 8.20–8.17 (m, 2H), 7.84 (td, 1H, $^3J = 7.8$ Hz, $^4J = 2.0$ Hz), 7.83 (s, 1H), 7.52–7.41 (m, 3H), 7.31 (ddd, 1H, $J = 7.4$ Hz, 4.9 Hz, 1.1 Hz), 3.59 (s, 2H), 2.32 (s, 6H); ^{13}C NMR ($CDCl_3$, 100 MHz) δ 156.8, 156.6, 155.9, 150.1, 149.2, 139.5, 137.0, 129.1, 128.8, 127.2, 123.8, 121.6, 120.6, 119.8, 63.7, 45.8; UV–vis (CH_2Cl_2) λ (nm) (ϵ , $M^{-1} cm^{-1}$) 304 (10600), 280 (14000), 261 (18600), 248 sh (20200), 240 (21700); IR (KBr, cm^{-1}) ν 3059 (w), 2973 (w), 2942 (w), 2813 (m), 2765 (m), 1583 (m), 1556 (m), 1406 (s), 1260 (m), 1043 (m), 885 (m), 774 (s), 735 (s); FAB $^+$ m/z (nature of the peak, rel intensity) 290.1 ($[M + H]^+$, 100). Anal. Calcd for $C_{19}H_{19}N_3$: C, 78.86; H, 6.62; N, 14.52. Found: C, 78.59; H, 6.42; N, 14.35.

4-(2-*p*-Tolylethynyl)-6-phenyl-2,2'-bipyridine (19): prepared, using procedure 2, from 4-iodo-6-phenyl-2,2'-bipyridine **15b** (400 mg, 1.11 mmol), *p*-tolylacetylene (200 μ L, 1.58 mmol), $[Pd(PPh_3)_2Cl_2]$ (88 mg, 0.12 mmol), CuI (21 mg, 0.11 mmol), THF (35 mL), and iPr_2NH (5 mL); chromatography on silica gel eluting with dichloromethane–petroleum ether (v/v 50/50 to 1/0); recrystallization from dichloromethane–petroleum ether to afford 270 mg (70%) of **19** as white crystals; 1H NMR ($CDCl_3$, 300 MHz) δ 8.72 (ddd, 1H, $J = 4.8$ Hz, 1.7 Hz, 0.8 Hz), 8.64 (d, 1H, $^3J = 7.9$ Hz), 8.51 (d, 1H, $^4J = 1.3$ Hz), 8.19–8.15 (m, 2H), 7.87 (d, 1H, $^4J = 1.3$ Hz), 7.86 (td, 1H, $^3J = 7.7$ Hz, $^4J = 1.8$ Hz), 7.56–7.43 (m, 5H), 7.34 (ddd, 1H, $J = 7.5$ Hz, 4.8 Hz, 1.1 Hz), 7.20 (d, 2H, $^3J = 7.9$ Hz), 2.40 (s, 3H); ^{13}C NMR ($CDCl_3$, 75 MHz) δ 156.8, 156.0, 155.9, 149.2, 139.5, 139.0, 137.0, 133.5, 132.0, 129.4, 129.3, 128.9, 127.1, 124.1, 122.1, 121.5, 121.4, 119.4, 94.0 ($C\equiv C$), 87.1 ($C\equiv C$), 21.7; UV–vis (CH_2Cl_2) λ (nm) (ϵ , $M^{-1} cm^{-1}$) 334 sh (7300), 310 (32800), 294 (37900), 264 (33000), 237 (27100); IR (KBr, cm^{-1}) ν 3059 (w), 2960 (w), 2935 (w), 2213 (m, $C\equiv C$), 1585 (m), 1538 (m), 1473 (m), 1393 (m), 1245 (m), 87 (m), 812 (s), 784 (s); FAB $^+$ m/z (nature of the peak, rel intensity) 347.2 ($[M + H]^+$, 100). Anal. Calcd for $C_{25}H_{18}N_2$: C, 86.68; H, 5.24; N, 8.09. Found: C, 86.52; H, 5.18; N, 7.92.

4-(2-(3,4,5-Tris(dodecyloxy)phenyl)ethynyl)-6-phenyl-2,2'-bipyridine (20): prepared, using procedure 2, from 4-iodo-6-phenyl-2,2'-bipyridine **15b** (215 mg, 0.60 mmol), 3,4,5-tris(dodecyloxy)-5-ethynylbenzene (400 mg, 0.61 mmol), $Pd(PPh_3)_2Cl_2$ (43 mg, 0.061 mmol), CuI (12 mg, 0.063 mmol), THF (35 mL), and iPr_2NH (5 mL); chromatography on silica gel eluting with dichloromethane–petroleum ether (v/v 25/75 to 80/20); reprecipitation from dichloromethane–methanol to afford 410 mg (77%) of **20** as light yellow

plates; 1H NMR ($CDCl_3$, 400 MHz) δ 8.71 (dt, 1H, $J = 3.8$ Hz, 1.0 Hz), 8.65 (d, 1H, $^3J = 8.0$ Hz), 8.50 (d, 1H, $^4J = 1.5$ Hz), 8.18–8.16 (m, 2H), 7.88–7.84 (m, 2H), 7.54–7.44 (m, 3H), 7.34 (ddd, 1H, $J = 7.4$ Hz, 4.9 Hz, 1.1 Hz), 6.80 (s, 2H), 4.03–3.99 (m, 6H), 1.87–1.73 (m, 6H), 1.51–1.46 (m, 54H), 0.90–0.87 (m, 9H); ^{13}C NMR ($CDCl_3$, 100 MHz) δ 156.8, 156.0, 153.2, 149.2, 139.9, 139.0, 137.1, 133.4, 129.4, 128.9, 127.1, 124.1, 121.9, 121.5, 121.4, 116.8, 110.6, 94.3 ($C\equiv C$), 86.5 ($C\equiv C$), 73.7, 69.3, 32.1, 32.0, 30.5, 29.9, 29.8, 29.7, 29.6, 29.5, 29.4, 26.2, 22.8, 14.3; UV–vis (CH_2Cl_2) λ (nm) (ϵ , $M^{-1} cm^{-1}$) 323 (31000), 286 (27300), 266 (31600), 254 (32900), 240 (35400); IR (KBr, cm^{-1}) ν 3054 (w), 2919 (s), 2849 (s), 2208 (m, $C\equiv C$), 1578 (m), 1500 (m), 1470 (m), 1394 (m), 1327 (m), 1239 (s), 1118 (s), 826 (m), 772 (m), 726 (m); FAB $^+$ m/z (nature of the peak, rel intensity) 886.0 ($[M + H]^+$, 100). Anal. Calcd for $C_{60}H_{88}N_2O_3$: C, 81.40; H, 10.02; N, 3.16. Found: C, 81.67; H, 10.27; N, 3.33.

(4-Iodo-6-phenyl-2,2'-bipyridine)chloroplatinum (23): prepared, using procedure 3, from 4-iodo-6-phenyl-2,2'-bipyridine **15b** (200 mg, 0.56 mmol), K_2PtCl_4 (255 mg, 0.61 mmol), acetonitrile (16 mL), and H_2O (8 mL); 229 mg (70%) of **23** obtained as an orange powder; 1H NMR ($(CD_3)_2SO$, 400 MHz) δ 8.81 (d, 1H, $^3J = 4.0$ Hz), 8.55–8.50 (m, 2H), 8.32–8.24 (m, 2H), 8.88 (t, 1H, $^3J = 6.5$ Hz), 7.58 (d, 1H, $^3J = 7.5$ Hz), 7.43 (d with ^{195}Pt satellites, 1H, $^3J = 7.5$ Hz), 7.14 (td, 1H, $^3J = 7.3$ Hz, $^4J = 1.3$ Hz), 7.05 (td, 1H, $^3J = 7.5$ Hz, $^4J = 1.0$ Hz); ^{13}C NMR ($(CD_3)_2SO$, 100 MHz) δ 165.2, 155.6, 154.6, 148.1, 145.8, 142.7, 140.4, 134.3, 130.6, 128.5, 127.9, 127.8, 125.3, 124.3, 123.9, 109.1; UV–vis (CH_2Cl_2) λ (nm) (ϵ , $M^{-1} cm^{-1}$) 438 (3500), 369 (7700), 334 (15200), 283 (35600), 270 sh (27800), 243 (30200); IR (KBr, cm^{-1}) ν 3057 (w), 1582 (m), 1532 (m), 1475 (m), 1405 (m), 1237 (m), 772 (s); FAB $^+$ m/z (nature of the peak, rel intensity) 553.0, 552.0, 551.0 ($[M - Cl]^+$, 60, 100, 80). Anal. Calcd for $C_{16}H_{10}ClIrPt$: C, 32.70; H, 1.72; N, 4.77. Found: C, 32.51; H, 1.47; N, 4.62.

(2-*p*-Tolylethynyl)(4-iodo-6-phenyl-2,2'-bipyridine)platinum (24): prepared, using procedure 4, from (4-iodo-6-phenyl-2,2'-bipyridine)chloroplatinum **23** (130 mg, 0.22 mmol), *p*-tolylacetylene (150 μ L, 1.18 mmol), CuI (4 mg, 0.02 mmol), DMF (25 mL), and triethylamine (5 mL); chromatography on aluminum oxide eluting with dichloromethane to give 103 mg (69%) of **24** as a dark red powder; 1H NMR ($(CD_3)_2SO$, 400 MHz) δ 8.98 (d, 1H, $^3J = 5.3$ Hz), 8.56 (s, 1H), 8.47 (d, 1H, $^3J = 8.0$ Hz), 8.31 (s, 1H), 8.28 (td, 1H, $^3J = 7.8$ Hz, $^4J = 1.5$ Hz), 7.82 (t, 1H, $^3J = 6.4$ Hz), 7.71 (d with ^{195}Pt satellites, 1H, $^3J = 7.2$ Hz), 7.60 (d, 1H, $^3J = 7.6$ Hz), 7.19 (Absys, 4H, $J_{AB} = 8.0$ Hz, $\nu_0\delta = 71.3$ Hz), 7.14–7.11 (m, 1H), 7.04 (t, 1H, $^3J = 7.6$ Hz), 2.30 (s, 3H); ^{13}C NMR ($(CD_3)_2SO$, 75 MHz) δ 164.1, 156.3, 154.6, 150.7, 145.9, 142.7, 139.8, 137.5, 133.9, 130.9, 130.8, 128.7, 128.6, 128.5, 127.6, 127.5, 125.8, 125.3, 124.4, 123.4, 109.1, 106.6 ($C\equiv C$), 105.2 ($C\equiv C$), 20.7; UV–vis (CH_2Cl_2) λ (nm) (ϵ , $M^{-1} cm^{-1}$) 470 (6300), 450 (6400), 377 (9600), 339 (14400), 284 (46000); IR (KBr, cm^{-1}) ν 3039 (w), 3012 (w), 2917 (w), 2850 (w), 2094 (m, $C\equiv C$), 1603 (m), 1578 (m), 1537 (m), 1500 (m), 1403 (m), 1240 (m), 1096 (m), 810 (s), 771 (s), 715 (s); FAB $^+$ m/z (nature of the peak, rel intensity) 669.1, 668.1, 667.1 ($[M + H]^+$, 80, 100, 75), 540.1 ($[M - I]^+$, 30). Anal. Calcd for $C_{25}H_{17}IrPt$: C, 44.99; H, 2.57; N, 4.20. Found: C, 44.68; H, 2.33; N, 3.87.

(2-*p*-Tolylethynyl)(4-(2-*p*-tolylethynyl)-6-phenyl-2,2'-bipyridine)-platinum (26): 4-Iodo-6-phenyl-2,2'-bipyridine)chloroplatinum **23** (80 mg, 0.136 mmol) and *p*-tolylacetylene (80 μ L, 0.63 mmol) were charged into a Schlenk tube with DMF (10 mL) and triethylamine (2 mL). The mixture was degassed by bubbling argon for 30 min, then $[Pd(PPh_3)_4]$ (34 mg, 0.029 mmol) was introduced and the reaction mixture stirred at room temperature for 42 h. The solvent was removed and the residue was treated with water and extracted with dichloromethane. The organic extracts were washed several times with water, then with saturated brine and filtered through hygroscopic cotton wool. After rotary evaporation the residue was purified by column chromatography on silica gel eluting with dichloromethane–petroleum ether (v/v 75/25 to 1/0). The residue

was reprecipitated in dichloromethane–cyclohexane to give 26 mg (30%) of **26** as a dark red solid; ^1H NMR (CDCl_3 , 400 MHz) δ 9.03 (dd, 1H, $^3J = 5.5$ Hz, $^4J = 1.0$ Hz), 7.94–7.89 (m, 2H), 7.79 (d, 1H, $^3J = 8.0$ Hz), 7.50–7.40 (m, 7H), 7.29–7.26 (m, 1H), 7.22 (d, 2H, $^3J = 8.0$ Hz), 7.14 (td, 1H, $^3J = 7.4$ Hz, $^4J = 1.3$ Hz), 7.08 (d, 2H, $^3J = 8.0$ Hz), 7.02 (td, 1H, $^3J = 7.5$ Hz, $^4J = 1.5$ Hz), 2.42 (s, 3H), 2.35 (s, 3H); ^{13}C NMR (CDCl_3 , 100 MHz) δ 165.0, 157.8, 154.4, 151.6, 146.4, 142.7, 140.3, 138.7, 138.6, 134.8, 134.1, 132.2, 131.8, 131.5, 129.5, 128.8, 127.6, 126.1, 124.6, 123.7, 123.0, 120.2, 120.0, 118.8, 106.9, 104.6, 97.3, 86.9, 21.9, 21.5; UV–vis (CH_2Cl_2) λ (nm) (ϵ , $\text{M}^{-1} \text{cm}^{-1}$) 478 (10600), 454 (10500), 374sh (15900), 339 (37200), 282 (51800), 249 (37000); IR (KBr, cm^{-1}) ν 3050 (w), 2209 (w, C \equiv C), 2088 (m, C \equiv C), 1596 (m), 1500 (m), 1400 (m), 1237 (m), 1018 (w), 862 (m), 814 (s), 778 (s); FAB $^+$ m/z (nature of the peak, rel intensity) 657.1, 656.1, 655.1 ($[\text{M} + \text{H}]^+$, 85, 100, 70), 540.0 ($[\text{M} - (\text{C}\equiv\text{C-tol})]^+$, 35). Anal. Calcd for $\text{C}_{34}\text{H}_{24}\text{N}_2\text{Pt}$: C, 62.28; H, 3.69; N, 4.27. Found: C, 61.92; H, 3.44; N, 3.89.

(2-*p*-Tolylethynyl)(4-(2-(3,4,5-tris(dodecyloxy)phenyl)ethynyl)-6-phenyl-2,2'-bipyridine)platinum (27): (2-*p*-Tolylethynyl)(4-iodo-6-phenyl-2,2'-bipyridine)platinum **24** (75 mg, 0.11 mmol) and 3,4,5-tris(dodecyloxy)-5-ethynylbenzene (98 mg, 0.15 mmol) were charged into a Schlenk tube with piperidine (15 mL). The mixture was degassed by bubbling argon for 30 min, then $[\text{Pd}(\text{PPh}_3)_4]$ (15 mg, 0.013 mmol) was introduced and the reaction mixture stirred at room temperature for 18 h. The solvent was evaporated and the residue purified by column chromatography on silica gel eluting with dichloromethane–petroleum ether (v/v 70/30). The product was reprecipitated in dichloromethane–methanol to give 62 mg (47%) of **27** as a red solid; ^1H NMR (CDCl_3 , 300 MHz) δ 8.88 (d, 1H, $^3J = 5.1$ Hz), 7.85 (dd with ^{195}Pt satellites, 1H, $^3J = 7.3$ Hz, $^4J = 0.9$ Hz), 7.79–7.69 (m, 2H), 7.45–7.41 (m, 3H), 7.31–7.23

(m, 2H), 7.14 (d, 1H, $^3J = 7.7$ Hz), 7.08–7.04 (m, 3H), 6.90 (td, 1H, $^3J = 7.5$ Hz, $^4J = 1.1$ Hz), 6.69 (s, 2H), 4.05–3.95 (m, 6H), 2.34 (s, 3H), 1.87–1.74 (m, 6H), 1.51–1.28 (m, 54H), 0.89 (t, 9H, $^3J = 6.7$ Hz); ^{13}C NMR (CDCl_3 , 75 MHz) δ 164.7, 157.6, 154.3, 153.3, 151.2, 146.4, 142.7, 140.5, 138.5, 138.4, 134.8, 133.8, 131.8, 131.3, 128.8, 127.3, 126.1, 124.6, 123.6, 123.2, 120.1, 119.9, 116.1, 110.8, 106.8, 104.9, 97.7, 86.4, 73.8, 69.4, 32.1, 30.6, 29.9, 29.8, 29.7, 29.6, 29.5, 26.3, 22.8, 21.5, 14.3; UV–vis (CH_2Cl_2) λ (nm) (ϵ , $\text{M}^{-1} \text{cm}^{-1}$) 478 (10900), 455 (10700), 361 (28100), 346 (28400), 283 (55100); IR (KBr, cm^{-1}) ν 3042 (w), 2919 (s), 2851 (s), 2207 (m, C \equiv C), 2102 (m, C \equiv C), 1601 (m), 1572 (m), 1504 (m), 1466 (m), 1364 (m), 1235 (s), 1116 (s), 1020 (m), 816 (m), 777 (m), 723 (m); FAB $^+$ m/z (nature of the peak, rel intensity) 1196.0, 1195.0, 1194.0 ($[\text{M} + \text{H}]^+$, 100, 95, 55), 1080.0 ($[\text{M} - (\text{C}\equiv\text{C-tol})]^+$, 30). Anal. Calcd for $\text{C}_{69}\text{H}_{94}\text{N}_2\text{O}_3\text{Pt}$: C, 69.38; H, 7.93; N, 2.35. Found: C, 69.19; H, 7.78; N, 2.07.

Acknowledgment. The authors thank the CNRS, the Ministère de la Recherche Scientifique, and the ANR FCP-OLEDs No. 05-BLAN-0004-01 for financial support. We are also indebted to Professor Jack Harrowfield (ISIS Strasbourg) for commenting on the manuscript prior to submission.

Supporting Information Available: General experimental procedure, reagents, materials, and experimental details for compounds **3**, **4**, **5**, **6**, **8**, **9**, **12**, **13**, **14**, **15**, **21**, **22**, and **25**, as well as CCDC numbers for X-ray structures of compounds **2a**, **2b**, **13**, **23**, and **24**. This material is available free of charge via the Internet at <http://pubs.acs.org>.

JO7019866